

# Decision-Feedback Closest Lattice Point Search for UMTS HSPA System

Byonghyo Shim, *Member, IEEE*, Farrokh Abrishamkar, and Insung Kang, *Member, IEEE*

**Abstract**—This letter considers a low-complexity multi-user detection based on the closest lattice point search (CLPS) for high speed packet access (HSPA) system. Instead of attempting to solve the ML detection problem in the presence of intersymbol and inter-cell interference, we utilize interference cancelled chips obtained from a bi-directional decision feedback operation to detect symbols. As a result, the worst case complexity of the CLPS is bounded to a controllable level irrespective of multipath spans. From the simulation on single and multi cell downlink communications in HSPA systems, we show that the proposed method offers substantial performance gain over conventional RAKE and MMSE equalizer.

**Index Terms**—Multi-user detection, interference cancellation, closest lattice point search, sphere decoding, high speed packet access.

## I. INTRODUCTION

Recently, increasing demand for high quality data services is fueling the deployment of high speed packet access (HSPA) mobile systems [1]. In order to support promised data rate in multi-user and multipath fading conditions, a strong receiver algorithm combatting the intercell interference (ICI) and inter-symbol interference (ISI) is critical. Traditionally, single-user detection methods such as RAKE and linear MMSE equalizer have long been employed, mainly due to their low complexity and implementation simplicity [2], [3]. While these schemes have been effective in mitigating the interference by averaging out chips with long spreading sequence, in HSPA system where such philosophy is not any more valid due to the short spreading factor (SF=16), a better strategy dealing with the interference is required.

In this letter, we propose a low-complexity multi-user detection (MUD) method, referred to as decision-feedback closest lattice point search (DF-CLPS) for the HSPA system. Exploiting the fact that the observation vector in a downlink is well modeled by a lattice corrupted by the noise, DF-CLPS searches the closest lattice point of the multi-user system. In searching this point, instead of performing ML detection to the matched filtered and whitened symbol vector [4], we utilize the interference cancelled chips obtained from a bi-directional decision feedback operation. As a result, maximum dimension

in CLPS is bounded to the SF irrespective of multipath spans so that the CLPS operation can be handled with a low complexity. An important step to make this approach possible is a two-stage preprocessing referred to as *causal cancellation* (CC) removing the postcursor ISI (ISI from the past symbols) and *non-causal cancellation* (NCC) cancelling both the precursor ISI (ISI from the future symbols) and the improved postcursor ISI. Due to the CC and NCC followed by the CLPS, while significantly reducing the computational complexity of the lattice point search, DF-CLPS achieves notably improved performance gain over conventional schemes in single and multi-cell downlink communication of HSPA in UMTS system.

## II. DF-CLPS

### A. Downlink System Model

The received signal vector for a downlink of HSPA system is given by

$$\mathbf{y} = \sum_i \mathbf{T}_i \mathbf{s}_i + \mathbf{v} = \sum_i \mathbf{H}_i \mathbf{C}_i \mathbf{W} \mathbf{G}_i \mathbf{s}_i + \mathbf{v} \quad (1)$$

where  $\mathbf{H}_i$ ,  $\mathbf{C}_i$ , and  $\mathbf{G}_i$  are the channel, scrambling code, and user gain matrices for a cell  $i$ ,  $\mathbf{W}$  is the Hadamard matrix (with SF=16), and  $\mathbf{T}_i = \mathbf{H}_i \mathbf{C}_i \mathbf{W} \mathbf{G}_i$  is the composite system matrix of cell  $i$ . In addition,  $\mathbf{s}_i$  is the symbol vector of users in a cell  $i$ ,  $\mathbf{v}$  is the white Gaussian noise vector having variance  $N_0$ , respectively. For our purpose, we define two SNR terms: 1) *geometry* defined as the power ratio between the target cell and all other interfering cells and 2) *target cell SNR* defined as the power ratio between the target cell and  $N_0$ .

When the multipath spans  $N_h$  chips, the length of  $\mathbf{y}$  becomes  $SF + N_h$ . Thus, chips corresponding to the previous and next symbols smear into those corresponding to the current symbol and thereby inducing an ISI. In this situation where the delay spread causes ISI, it is instructive to divide the composite system matrix  $\mathbf{T}_i$  into three submatrices:  $\mathbf{T}_i^{n,l}$ ,  $\mathbf{T}_i^n$ , and  $\mathbf{T}_i^{n,r}$ , each of which represents the effective channel for previous, current, and next symbols ( $\mathbf{s}_i^{n-1}$ ,  $\mathbf{s}_i^n$ , and  $\mathbf{s}_i^{n+1}$ ) in a cell  $i$ . With this notation, (1) can be rewritten as

$$\mathbf{y}_n = \sum_i \left( \mathbf{T}_i^{n,l} \mathbf{s}_i^{n-1} + \mathbf{T}_i^n \mathbf{s}_i^n + \mathbf{T}_i^{n,r} \mathbf{s}_i^{n+1} \right) + \mathbf{v}_n. \quad (2)$$

where we have used  $\mathbf{y}_n$  in order to stress the dependency of observation vector on symbol time  $n$ . In this letter, we focus on the case where  $N_h \leq SF$  for simplicity. However, the extension to the case where  $N_h > SF$  would be straightforward by considering additional interference terms caused by  $\mathbf{s}_i^{n-2}$  and  $\mathbf{s}_i^{n+2}$ .

Copyright (c) 2008 IEEE. Personal use of this material is permitted. However, permission to use this material for any other purposes must be obtained from the IEEE by sending a request to pubs-permissions@ieee.org.

B. Shim is with the School of Information and Communication, Korea University, Seoul, 136-713, Korea (e-mail: bshim@korea.ac.kr).

F. Abrishamkar and I. Kang are with Qualcomm Inc., San Diego, CA, 92121, USA (e-mail: {farrokha,insungk}@qualcomm.com).

This work is supported by a research grant from Qualcomm Inc. and KOSEF R01-2008-000-20292-0.

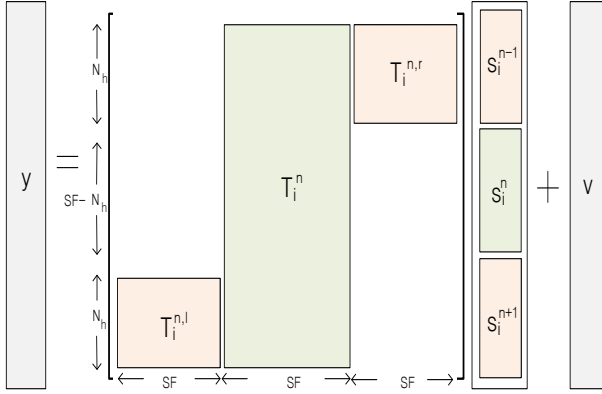


Fig. 1. Received signal structure for the HSPA downlink with a single cell transmission when  $N_h \leq SF$ .

### B. Single Cell Scenario

If a mobile is located near the base-station so called node-B, only a single cell would be dominant due to high geometry and target cell SNR and hence (2) is approximately

$$\mathbf{y}_n \approx \mathbf{T}_i^{n,l} \mathbf{s}_i^{n-1} + \mathbf{T}_i^n \mathbf{s}_i^n + \mathbf{T}_i^{n,r} \mathbf{s}_i^{n+1} + \mathbf{v}_n. \quad (3)$$

In detecting  $\mathbf{s}_i^n$ , the spillover from adjacent symbols should be considered since otherwise the potential gain will be significantly reduced. In this respect, the optimal ML formulation should include adjacent symbols and thus

$$\hat{\mathbf{s}}_i^n = \arg \min_{\{\mathbf{s}_i^n, \mathbf{s}_i^{n-1}, \mathbf{s}_i^{n+1}\} \in \mathcal{X}^{3SF}} \|\mathbf{y}_n - \mathbf{T}_i^n \mathbf{s}_i^n - \mathbf{T}_i^{n,l} \mathbf{s}_i^{n-1} - \mathbf{T}_i^{n,r} \mathbf{s}_i^{n+1}\|^2 \quad (4)$$

where  $\mathcal{X}$  is the set of all possible constellation point. This means that the ML formulation should include full vestige of previous and next symbols to minimize their spillover on the current symbol. It should be emphasized that it is impractical, even with an efficient CLPS algorithm so called sphere decoding (SD) [5], to find  $\hat{\mathbf{s}}_i^n$  since the total number of lattice points is astronomical (recall that the SF of data channel in HSPA is 16 and each channel supports upto 64-QAM modulation [1],  $|\mathcal{X}|^{3SF} = 64^{48} \approx 5 \cdot 10^{86}$ ).

In the proposed method, instead of attempting to solve (4), we obtain a linear system related only to the current symbol  $\mathbf{s}_i^n$  and then solve it using the CLPS algorithm. The key idea of the proposed DF-CLPS lies on the cancellation of postcursor and precursor ISI using causal and non-causal decision feedback processing. Note that within the observation duration of  $\mathbf{y}$ , i.e., during  $SF + N_h$  chip time, the first  $N_h$  chips contain the postcursor ISI and the last  $N_h$  chips contain the precursor ISI as illustrated in Fig. 1. The postcursor ISI is cancelled first in the CC stage and the precursor ISI as well as improved postcursor ISI are cancelled next in the NCC stage.

In the CC stage, the modified observation after cancelling out the postcursor ISI becomes

$$\mathbf{y}'_n = \mathbf{y}_n - \mathbf{T}_i^{n,l} \mathbf{s}_i^{n-1} = \mathbf{T}_i^n \mathbf{s}_i^n + \mathbf{T}_i^{n,r} \mathbf{s}_i^{n+1} + \tilde{\mathbf{v}}_n \quad (5)$$

where  $\tilde{\mathbf{v}}_n$  contains the original noise  $\mathbf{v}$  as well as the cancellation error due to incorrectly detected  $\hat{\mathbf{s}}_i^{n-1}$ . If the previously detected symbol  $\hat{\mathbf{s}}_i^{n-1}$  is error-free, the half of ISI is erased so that the received SINR is changed from  $\frac{P_s}{I_{n-1} + I_{n+1} + N_0}$  to  $\frac{P_s}{I_{n+1} + N_0}$  where  $P_s = E[|\mathbf{T}_i^n \mathbf{s}_i^n|^2]$ ,  $I_{n-1} = E[|\mathbf{T}_i^{n,l} \mathbf{s}_i^{n-1}|^2]$ ,  $I_{n+1} = E[|\mathbf{T}_i^{n,r} \mathbf{s}_i^{n+1}|^2]$ . In a high geometry scenario where  $I_{n-1}, I_{n+1} \gg N_0$  and noting also that  $I_{n-1} \approx I_{n+1}$ , we have  $\frac{P_s}{I_{n-1} + I_{n+1} + N_0} \approx \frac{1}{2} \frac{P_s}{I_{n+1} + N_0}$  resulting in almost 3 dB gain in SINR.

The detection in the CC stage is performed via the CLPS given by

$$\hat{\mathbf{s}}_i^n = \arg \min_{\mathbf{s}_i^n \in \mathcal{X}^{SF}} \|\mathbf{y}'_n - \mathbf{T}_i^n \mathbf{s}_i^n\|^2. \quad (6)$$

We mention that this CLPS problem is by no means equivalent to the ML detection problem due to the non-Gaussian nature of the effective noise including precursor ISI and detection errors of the postcursor ISI [6]. In spite of this, by employing the SD algorithm searching the hypersphere  $\|\mathbf{y}'_n - \mathbf{T}_i^n \mathbf{s}_i^n\|^2 < d_0$ , the closest lattice point  $\hat{\mathbf{s}}_i^n$  can be obtained. We skip the detail of the SD algorithm in this letter, but mention that the SD algorithm avoids an exhaustive search over all possible lattice points by performing a constrained lattice point search within a hypersphere with a small radius [5], [6].

The NCC operation is performed in parallel with the CC operation but with different symbol time. While the CC stage processes  $\mathbf{s}_i^n$  at symbol time  $n$ , the NCC stage moves two symbol time back to the past and computes the estimate of  $\mathbf{s}_i^{n-2}$ . In order to distinguish the NCC output from the CC output, we use  $\tilde{\mathbf{s}}_i^{n-2}$  for the NCC estimate. Since  $\tilde{\mathbf{s}}_i^{n-3}$  is available from the previous NCC operation and  $\hat{\mathbf{s}}_i^{n-1}$  is also available from the previous CC operation, the postcursor and precursor ISI can be removed as

$$\begin{aligned} \mathbf{y}''_{n-2} &= \mathbf{y}_{n-2} - \mathbf{T}_i^{n-2,l} \underbrace{\tilde{\mathbf{s}}_i^{n-3}}_{\text{from NCC}} - \mathbf{T}_i^{n-2,r} \underbrace{\hat{\mathbf{s}}_i^{n-1}}_{\text{from CC}} \\ &= \mathbf{T}_i^{n-2} \mathbf{s}_i^{n-2} + \tilde{\mathbf{v}}_{n-2} \end{aligned} \quad (7)$$

where  $\tilde{\mathbf{v}}_{n-2}$  consists of  $\mathbf{v}_{n-2}$  and the cancellation error due to incorrectly detected  $\hat{\mathbf{s}}_i^{n-3}$  and  $\hat{\mathbf{s}}_i^{n-1}$ . Using the modified observation  $\mathbf{y}''_{n-2}$ ,  $\mathbf{s}_i^{n-2}$  is re-detected via CLPS given by

$$\tilde{\mathbf{s}}_i^{n-2} = \arg \min_{\mathbf{s}_i^{n-2} \in \mathcal{X}^{SF}} \|\mathbf{y}''_{n-2} - \mathbf{T}_i^{n-2} \mathbf{s}_i^{n-2}\|^2. \quad (8)$$

The overall timeline of CC and NCC operation is summarized in Table I.

### C. Multiple-Cell Scenario

When the mobile is located near the boundary of a cell, the single-cell approximation in (3) is no longer valid and thus multiple cell information should be employed to obtain the best result. Since the ICI is a dominant impediment in this scenario, we control it by performing the cell-based CC and NCC operation in a sequential order. In fact, we sort cells in their power (usually measured by the pilot channel power) and then perform the CC and NCC operation using this order. In contrast to the single-cell scenario where major operations are the ISI cancellation and the CLPS, the multi-cell CC and

TABLE I  
TIMELINE OF CC AND NCC OPERATIONS FOR THE SINGLE CELL SCENARIO

symbol time	n	n+1
CC observation	$\mathbf{y}'_n = \mathbf{y}_n - \mathbf{T}_i^{n,l} \hat{\mathbf{s}}_i^{n-1}$	$\mathbf{y}'_{n+1} = \mathbf{y}_{n+1} - \mathbf{T}_i^{n+1,l} \hat{\mathbf{s}}_i^n$
CC output	$\hat{\mathbf{s}}_i^n$	$\hat{\mathbf{s}}_i^{n+1}$
NCC observation	$\mathbf{y}''_{n-2} = \mathbf{y}_{n-2} - \mathbf{T}_i^{n-2,l} \hat{\mathbf{s}}_i^{n-3} - \mathbf{T}_i^{n-2,r} \hat{\mathbf{s}}_i^{n-1}$	$\mathbf{y}''_{n-1} = \mathbf{y}_{n-1} - \mathbf{T}_i^{n-1,l} \hat{\mathbf{s}}_i^{n-2} - \mathbf{T}_i^{n-1,r} \hat{\mathbf{s}}_i^n$
NCC output	$\hat{\mathbf{s}}_i^{n-2}$	$\hat{\mathbf{s}}_i^{n-1}$

NCC have an additional step for ICI cancellation referred to as a retransmitted chip cancellation. Specifically, when the symbol vector  $\mathbf{s}_i^n$  is detected, we perform the retransmission to obtain the retransmitted chip  $\mathbf{T}_i^n \mathbf{s}_i^n$  and then cancel this from the observation. In doing so, when the CC and NCC operations is finished, all of the user's signals and interferences are removed. For the re-detection of symbols in a cleaned environment, we thus need to add back the retransmitted chip of the symbols. Indeed, the CLPS is performed after canceling all possible interferences so that the CLPS problem of the CC stage is

$$\hat{\mathbf{s}}_i^n(k) = \arg \min_{\mathbf{s}_i^n \in \mathcal{X}^{SF}} \|\mathbf{y}' - \mathbf{T}_i^n \mathbf{s}_i^n\|^2 \quad (9)$$

where  $\mathbf{y}'_n$  is given by

$$\begin{aligned} \mathbf{y}'_n = \mathbf{y}_n - \sum_j \mathbf{T}_j^{n,l} \hat{\mathbf{s}}_j^{n-1}(k) \\ - \left( \sum_{j < i} \mathbf{T}_j^n \hat{\mathbf{s}}_j^n(k) + \sum_{j > i} \mathbf{T}_j^n \hat{\mathbf{s}}_j^n(k-1) \right). \end{aligned} \quad (10)$$

It is worth pointing out that all symbol estimates are the most recent estimates. That is, depending on the order of estimation, some estimates are from the initial detection ( $k = 0$ ) and others are from the re-detection ( $k = 1$ ). If we interpret  $k$  as an iteration index, further iteration ( $k > 1$ ) is of course possible but the additional performance improvement would be marginal as  $k$  increases.

In a similar manner, the CLPS of the NCC operation is given by

$$\hat{\mathbf{s}}_i^n(k) = \arg \min_{\mathbf{s}_i^n \in \mathcal{X}^{SF}} \|\mathbf{y}'' - \mathbf{T}_i^n \mathbf{s}_i^n\|^2 \quad (11)$$

where  $\mathbf{y}''_n$  is

$$\begin{aligned} \mathbf{y}''_n = \mathbf{y}_n - \sum_j \mathbf{T}_j^{n,l} \hat{\mathbf{s}}_j^{n-1}(k) \\ - \left( \sum_{j < i} \mathbf{T}_j^n \hat{\mathbf{s}}_j^n(k) + \sum_{j > i} \mathbf{T}_j^n \hat{\mathbf{s}}_j^n(k-1) \right) - \sum_j \mathbf{T}_j^{n,r} \hat{\mathbf{s}}_j^{n+1}(k). \end{aligned} \quad (12)$$

### III. SIMULATIONS RESULTS AND DISCUSSION

In our simulation, we tested the performance of the proposed method in HSPA (release 7) of UMTS standard [1], where the downlink signal is transmitted from two asynchronously operated cells (i.e., target and interfering cells) in a multipath environment. The simulated propagation channels have three distinct multipaths and the relative powers for each path are 0, -6, and -9 dB, respectively ( $h[n] = 0.852\delta[n] + 0.427j\delta[n-1] - 0.302\delta[n-2]$ ). Both desired user in a target cell as well as interferer in a secondary cell employ five data channels (HS-PDSCH). The modulation scheme of interferer

is fixed with QPSK while that of the target cell user can switch between QPSK and 16-QAM per 2 ms transmission time interval (TTI) depending on the channel condition. As a performance metric, we employed the symbol error rate (SER) of data channels in a target cell. For each point in the SER curve, we simulated at least 1000 TTI.

We first considered the single-cell scenario with geometry 20 dB so that the target cell is dominant over the interfering cell. Notice that this scenario represents the situation where a mobile is located close to the node-B so that target user receives 16-QAM modulated data symbols. In order to obtain a comprehensive view, we tested conventional methods (RAKE and linear MMSE equalizer) as well as proposed approaches (CLPS only, CC-CLPS, and NCC-CLPS). Note that while the method denoted as CLPS only performs the CLPS of the current symbol vector, CC-CLPS and NCC-CLPS perform the additional postcursor ISI and post/precursor ISI cancellation, respectively.

As shown in Fig. 2, even the CLPS searching only current symbols provides considerable performance gain over conventional methods resulting in more than 2 dB gain at SER of  $10^{-1}$  compared to the linear MMSE equalizer. Due to the postcursor cancellation, we observed that the CC-CLPS provides a noticeable performance improvement over the CLPS method. In particular, the amount of improvement increases fast in high target cell SNR regime where the interference dominates noise power so that the gain is close to 4 dB at SER of  $10^{-2}$ . Further, by employing the NCC-CLPS, we could obtain additional considerable gain from the improved postcursor cancellation and the precursor cancellation.

Next, we considered the multi-cell scenario modeling the mobile located in a cell boundary. In this case, we set -3 dB geometry and thus the ICI is major impediment to the mobile. Due to the ICI, modulation format of the data channel in this scenario is changed to QPSK. As shown in Fig. 3(a), the receiver performance is in general worse than the single-cell scenario. Since the proposed methods perform the CLPS operation after the ICI cancellation, performance improvement over the linear MMSE equalizer is noticeably better than the single-cell scenario. In order to observe if this gain can be transferred to the gain after decoding, we simulated the system using UMTS standard half-rate ( $r = 1/2$ ) turbo code with  $g_0(D) = 1 + D^2 + D^3$  and  $g_1(D) = 1 + D + D^3$  [1]. The code block size is set to 4800 and 5 iterations are performed for each code block in the receiver. In generating the log-likelihood ratio (LLR) of proposed methods, we employ  $\hat{s} = s + n$ ,  $n \sim \mathcal{N}(0, \sigma_n^2)$  model since the CLPS operation returns hard-

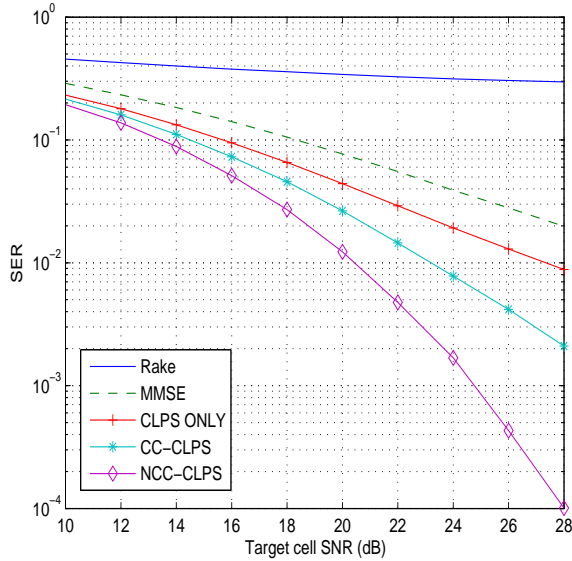


Fig. 2. SER performance of proposed approaches in a single-cell scenario.

decided outputs. The corresponding LLR is given by

$$L(b_k) = \log \frac{\sum_s \exp(-(\hat{s} - s_{b_{k+}})^2 / 2\sigma_n^2)}{\sum_s \exp(-(\hat{s} - s_{b_{k-}})^2 / 2\sigma_n^2)} \quad (13)$$

where  $s_{b_{k+}}$  is the symbol generated by  $b_k = +1$  ( $s_{b_{k-}}$  is defined in the similar way) and  $\sigma_n^2$  is the cost function (normalized by the number of channels) of the CLPS operation. Fig. 3(b) compares the BER performance after the decoder for each method. Although the performance of CLPS and CC-CLPS is slightly worse than the linear MMSE equalizer in very low SNR regime, we observe that the performance improvement of proposed methods is pronounced for mid and high SNR regime. In fact, as the SNR increases, the interference cancellation of the proposed methods becomes more accurate and thus the gain over the conventional schemes becomes larger.

In this work, we discussed a low-complexity MUD method for UMTS HSPA system, based on the non-causal interference cancellation and the CLPS. Although the complexity of the SD algorithm which clearly is a major building block of the DF-CLPS might be a bottleneck for the implementation, we would like to indicate that the recent advances in near ML lattice detection algorithms [7] can bring significant reduction in complexity at the expense of graceful performance degradation.

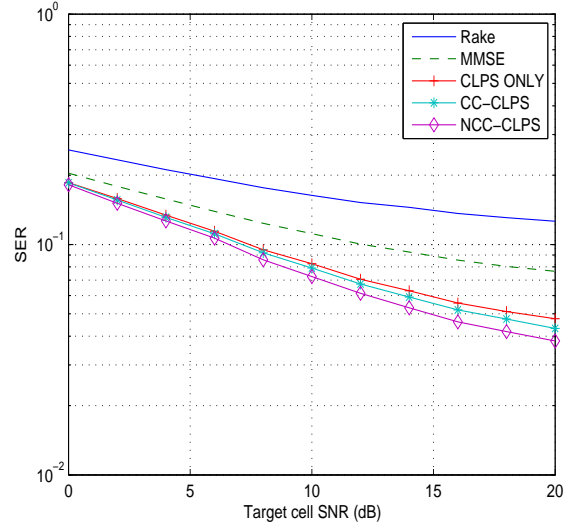
REFERENCES

[1] "3rd Generation Partnership Project: Technical specification group radio access network; physical layer (Release 7)," Tech. Spec. 25.201 V7.2.0, 2007. (see [http://www.3gpp.org/ftp/Specs/archive/25\\_series/25.201/25201-720.zip](http://www.3gpp.org/ftp/Specs/archive/25_series/25.201/25201-720.zip)).

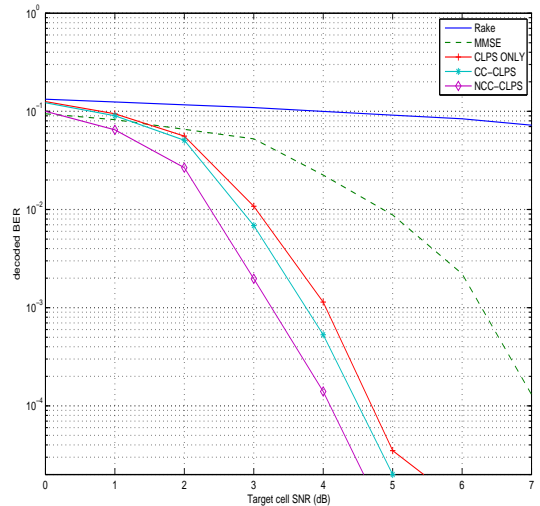
[2] S. Verdu, *Multuser detection*, Cambridge Univ. Press, 1998.

[3] S. Moshavi, "Multi-user detection for DS-CDMA communications," *IEEE Comm. Magazine*, pp. 124-136, Oct. 1996.

[4] L. Brunel and J. J. Boutros, "Lattice decoding for joint detection in direct-sequence CDMA systems," *IEEE Trans. Inf. Theory*, vol. 49, pp. 1030-1037, April 2003.



(a)



(b)

Fig. 3. Performance of proposed approaches in a two-cell scenario. (a) SER and (b) BER after decoder.

[5] U. Fincke and M. Pohst, "Improved methods for calculating vectors of short length in a lattice, including a complexity analysis," *Mathematics of Computation*, vol. 44, pp. 463-471, 1985.

[6] M. O. Damen, H. E. Gamel, and G. Caire, "On maximum-likelihood detection and the search for the closest lattice point," *IEEE Trans. Inf. Theory*, vol. 49, pp. 2389-2402, Oct. 2003.

[7] B. Shim and I. Kang, "Sphere decoding with a probabilistic tree pruning", *IEEE Trans. Signal Process.*, vol. 56, pp. 4867-4878, Oct. 2008.